EAI Endorsed Transactions
on Energy Web
Research Article EAI.EU

Performance Investigation of HFR Full-bridge Inverter in Resonant Inductive Coupled Power Transfer System for an Electric Vehicle

P. Geetha[1] and S. Usha[1,*]

[1]Department of Electrical and Electronics Engineering, SRM Institute of Science and Technology, Kattankulathur, Chennai, 603203, India

Abstract

Inductive WPT of the resonant category is generally employed for medium and high-power transmission applications like electric vehicle charging due to it contributes excellent efficiency. The high-frequency resonant full-bridge inverter using series-series resonant topology is proposed. The design of the high-frequency resonant inverter is simulated and verified by MATLAB/SIMULINK software. The charging scheme which is available in the AC-DC as well as in the DC-DC converter should operate with the two steps to achieve a duty cycle-based voltage control and hysteresis current control. The resonant frequency of the proposed system has a frequency range of 65 kHz with a DC voltage of 12V. The simulation has been carried out successfully and transmitted a 5KW power load of constant current and voltage control. The Performance chart of with the existing method is carried out in terms of parameters and the efficiency can be achieved by 95%.

Keywords: Wireless Charging Technique method in the Electric Vehicle, Battery Charging type, Resonant Inductively Coupled Power Transfer, High-frequency inverter, Wireless Power Transmission (WPT)

Received on 03 December 2023, accepted on 21 February 2024, published on 28 February 2024

doi: 10.4108/ew.5227

*Corresponding author. Email: ushas@srmist.edu.in

1. Introduction

Currently, the development of electric vehicles which have been encountering excellent results in decreasing the various types of vehicle radiation concerns along with the growing economy part in the present generation. This environmental-impelled result, although is facing an irresistible threat at some of the components: cost and well-defined driving area [1]. Both prices of EVs and limited concern are well-permitted as important obstacles that block EVs from development and mass acceptance [2]. Hence, some conditions on some results performed, WPT is encountered as an auspicious concept to improve the EV's charging system for its scientific furtherance and improvement. WPTs may respond to the issue through the domain of the very small propulsion anxiety selection, the amount of time required to power the vehicular system in an extended period, along with the expense and range of the vehicle system's charging infrastructure is more effective than no other options, which include swapping batteries, frequent and quick conductive charging. Hence, it further provides much more good protection and good comfort for electric vehicle users [3].

In Resonant inductive power transfer, the longitudinal is arranged such a way as to produce the dipole fields. The dipole field decreases as decreases due to the cube of the distance between the coils of a transmitter (main) and the receiver (secondary). Thus, the distance between two coils is the major factor affecting the efficiency. Thus, when the coils of a receiver and the transmitter will be very close in contact then the efficiency range will have a better performance [4],[5].

Resonant inductive coupling mainly contains magnetic fields for transmitting power and hence it is called 'Magnetic coupling'. The resonant inductive coupling contains the electromagnetic field with the combination of an electric circuit to generate an Electro Motive Force (EMF) in the secondary coil and it mainly depends on Faraday's law of induction principle [6]. Thus, the power transmission that occurs in the resonant inductive coupling is proportional to the mutual inductance which is present in between the two coils, and it is suitable for high frequency also [7]. The mutual inductance of the coils in the inductive coupling of the transmitter and receiver is expressed in the equation given as

$$M = k \, x \sqrt{(L_1 x L_2)} \quad (1)$$

Where, k is the dimensionless parameter, and it is a coupling coefficient.

When compared to the quick development, huge mobility information technology, and penetration, a WPT is now waiting for the occurrence of conductive energy transmission [8]. So, there should be comprehensive layout designs with resonant inductively coupled wireless power transmission systems that include the vehicle battery charging systems and the factory conveyance systems then their efficiency is acceptable up to the range of 80% has been noted [9],[10].

Many kinds of research have been neglected to find out the very nearer range and many layouts' structures report to the magnetic materials to enhance and develop the boost energy power transmission for selecting the magnetic flux in a minimum loss path [11],[12]. EV charging is mainly carried out by the method of resonant inductive Power Transfer. When compared to another method the inductive coupling method is more prominent and provided a secure and steady form for the electric vehicle charging wireless and when compare with the technique called near-fields is the capacitive coupling or magnetic resonance coupling [13]. Thus, this may be considered a growing universal aspect so that research experts and factories from all over the people across the world are cordially joining together for the improvement of electric vehicle technology [14]. In the latest research published by the wireless power transmission Research Group of the Institute Technology of Bandung [15], the research group is having the proposed circuit model for the simulations with a compensating topology of a series-parallel type that contains and offered a greater convenience method for the entire circuit [16]. The specification for the parameters and particulars of the transfer electric circuit will resolve and find out the power converters which can be applied to encourage and promote this inductive coupling method [17].

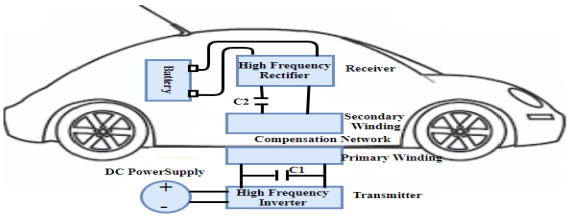

Figure 1. Configuration of the EV wireless charging system

The primary goal of this research is to design, layout, simulate, modulate, and evaluate an HF Resonant Full Bridge Inverter using a method called resonant inductive wireless power transmission system for electric vehicles to consolidate and coordinate with the DC networks and topologies used [18]. Then, they have the main advantages like developing the system performance parameters when relatively compared to traditional EV charging systems. To tackle this drawback of IPT the WPT system of the IPT can be combined with the resonant circuits. Figure 1 depicts the configuration of the wireless charging system. Thus, for the resonant circuits, the supply switching frequency is designed and is equalized with the resonant frequency and when the system is in the condition of resonance state then it allows for producing a very high maximum performance [19]. This kind of system will make use of that and target to improve a system parameter with better-enhanced system performance. The proposed circuit diagram is designed and verified by using the software MATLAB/SIMULINK to get good system performance. The component's values are evaluated by deriving the equations for every component present.

This paper will show the steps for how to evaluate the better options for the converters present on both the transmitter and receiver sides. Wireless power transfer is a developing technology for the modern generation. Nowadays, many electrical equipment companies have introduced an economic usage of wireless charging applications in smartphones, EV trains and cars, and many other electronic gadgets. WPT plays a vital role in the healthcare sector, used mainly in implantable medical devices. In this paper, the high-frequency resonant full-bridge inverter using series-series resonant topology is proposed. The process is divided into three main divisions namely a full-bridge inverter present in the transmitter coil with the frequency modulation having a high-frequency power contribution, a linear three windings transformer that coordinates with the series-series resonant RLC topology for both primary and secondary windings. The proposed output circuit can be rectified by using a high-frequency rectifier on the receiver side. The entire primary switches of an EV battery charging method can allow the usage of resistance power in low on-state switching MOSFETs to obtain maximum efficiency in the high-frequency range. This paper represents a simplified simulation type that should be used for smartphones, and EV cars with a massive efficiency range of 95% and will be fixed nearby. The 5-kW dynamic wireless power transmission system is generated and

verified to test the major aspect of an electric vehicle. In this paper, section I consists of an introduction to the WPT of its advantages and its disadvantages. After that Section II contains the system design and the simulation of the proposed method. Then Section III part contains the result and its discussion of the proposed simulation method. Section IV contains the conclusion of the proposed method and its future work.

2. System design and simulation

2.1 Proposed method of wireless charging system

The normalized structure of a wireless charging system of an EV is shown in this paper, and it is depicted in Figure 2. The outside of the vehicle presents on the primary side and consists of a DC power supply, a high-frequency H- bridge MOSFET inverter (Power Electronics), along with the primary winding connected to the transmitter coil of the high-frequency transformer. The secondary side called as power pickup system of the receiver, the side is fixed inside the vehicle, and it consists of the converter, high-frequency rectifier, and filtering capacitor, DC output voltage. Then the EV on board battery is to be charged wirelessly. Thus, in the resonance state condition, the EV wireless charging system can operate precisely in coordination with the compensation topologies such as the capacitance of the primary as C_p and the capacitance of the secondary as C_s. It is present in the transmitter and the receiver sides of an EV wireless charging system.

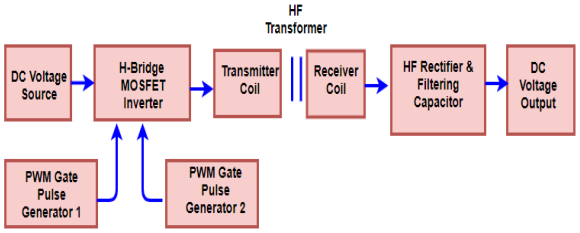

Figure 2. Wireless power transmission system

Transmitter

On the transmitter side the Dc voltage supply is given to the high-frequency H-Bridge MOSFET inverter. The HF inverter used here is a half-bridge push-pull type inverter. It is operated using a PWM switching controller which produces 45 to 120 kHz oscillator Frequency. The HF converter converts Dc to HF ac. The HF AC is fed to a switching transformer, which drives the HF Ac power to the transmitting coil. Transmitting coils convert HF electrical current into electromagnetic waves. The transmitting (main) coil is operated at its condition of resonant frequency so that maximum power will be transmitted with higher output efficiency.

Receiver

On the receiver side, it consists of a receiving coil it is tuned to the frequency of the transmitting coil. So, when coils are within the coupling range, the power is received in the receiving coil. In that electromagnetic waves are converted back to HF AC. A fast-switching full bridge rectifier is present in the output of the receiving coil, and it is interconnected, which converts the given HF current into a DC voltage output. A DC-DC converter is used on this coil's side, which stabilizes the input DC voltage and produces a constant DC output. The proposed block diagram is shown in Figure 2, which analyze and it is based on the following design equation.

2.2 Evaluation of inductive power transmission

Series resonant power transmission

A typical square-wave inverter of the source voltage is selected for the transmitted-end converter, as a result, the downstream resonant type transmitted by the network present in the minimum input DC voltage should be fully undergone testing and it may be used. Figure 3 shows the steps involved in the simulation design in the overview of a flowchart. Thus, the series-type resonant power transmission topology is selected because of their improved type of current limiting, a series connection is linked with the variable impedance and then the resonance frequency equation is equated as,

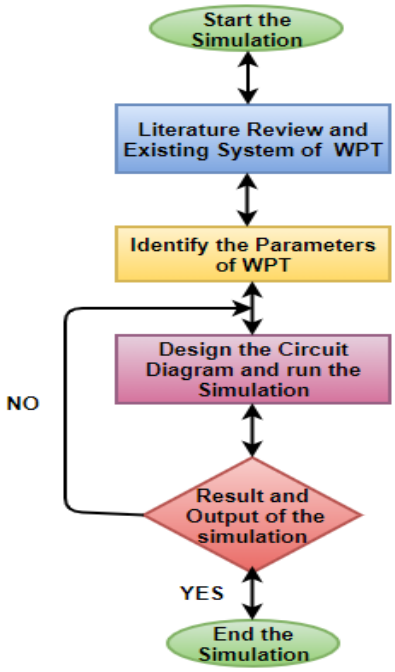

Figure 3. Flow chart of the proposed method

$$fr = \frac{1}{2\pi\sqrt{L1C1}} = \frac{1}{2\pi\sqrt{L2C2}} \quad (2)$$

$L_{1,2}$ and $C_{1,2}$ are considered as series inductance and series capacitance that includes leakage appropriately. A comprehensive simplified form of the Series-Series type

(SS) resonant topology circuit diagram is depicted in Figure 4, here T equivalent circuit is analyzed in the main coil which is present in the transmitter by the self-inductance and the coil of the receiver also. In this equivalent circuit diagram of this topology, where M represents the mutual inductance, Resistance 1, and Resistance 2 are used in this circuit diagram as an equivalent series resistance (ESR) for the coil present in the inductor and resonant capacitor. The simplified circuit of the AC analysis test is done, and the value of the efficiency can be obtained in Equation (2) and this can be obtained by applying the primary and secondary current (I1 and I2) in Equation (3).

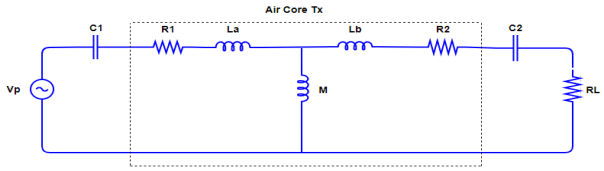

Figure 4. Series-series type resonant topology

Thus, it may be noticed from the above equation, that the efficiency value of the transfer energy is normally linked with the factor of coupling and the resonant quality network. Then Equation (4) is used to obtain the maximum efficiency of the resonant network. If case the squares of the operating frequency are adequately greater than the terms and the equation is given as follows,

$$\frac{R_1(R_L+R_2)}{M^2} \tag{3}$$

$$\eta=\frac{I_2^2R_L}{I_p^2R_1+I_2^2R_2+I_2^2R_L}=\frac{R_L}{R_L+R_2\left[1+\frac{R_1(R_L+R_2)}{\omega_R^2M^2}\right]} \tag{4}$$

$$\frac{I_1}{I_2}=\frac{R_2+R_L}{\omega_0 M} \tag{5}$$

$$\eta_{max}=\frac{R_L}{R_2+R_L} \tag{6}$$

In the above equation (4), from this equation, the maximum efficiency can easily find out and it is mainly based on the parameters such as the secondary side of the parasitic resistance parameters specifications and another one is the load resistance. Hence, normally the resistance present in the load is very much higher than the secondary side of the parasitic resistance, then the analytical efficiency is maximum, hence we may interpret that the deviation of the load might not change the efficiency considerably.

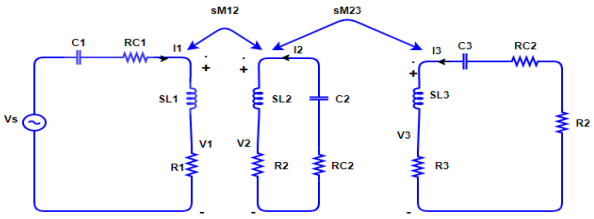

Figure 5. Equivalent circuit diagram of series resonant

Figure 5 depicts a simplified Equivalent circuit diagram for the wireless power transmission system having parameters in the lumped structure for both sides of the transmitter and receiver. Thus, the following equations are derived from Figure 7 as shown below.

The quality factor is expressed, and the equation is given by

$$Q=\frac{\omega_0 L}{R}=\frac{1}{\omega_0 CR}=\frac{1}{R}.\frac{\sqrt{L}}{C} \tag{7}$$

$$g_{32\_S}=\frac{i_3}{i_2}=-\frac{j\omega L_{M23}}{j\omega L_3+R_3+R_{C2}+\left(\frac{1}{j\omega C_2}\right)+R_L} \tag{8}$$

$$g_{21\_S}=\frac{i_2}{i_1}=-\frac{j\omega L_{M12}}{j\omega L_2+R_2+R_{C2}+\left(\frac{1}{j\omega C_2}\right)+j\omega L_{M23}*g_{32}} \tag{9}$$

$$i_1=\frac{V_S}{j\omega L_1+R_1+R_{C3}+\left(\frac{1}{j\omega C_1}\right)+j\omega L_{M12}*g_{21}} \tag{10}$$

$$P_{0\,S}=|i_3|.R_L=|Dg_{32}g_{21}i_1| \tag{11}$$

By applying Kirchhoff's law of Voltage (KVL), then the resonant circuit's differential equations for the second order can be evaluated and the equations for the second-order equations be given as follows

$$LC\frac{d^2i_L}{dt}+RC\frac{di_L}{dt}+i_L=0 \tag{12}$$

3. Results and discussions

In this article, the HF Resonant Full Bridge Inverter using series resonant topology is simulated using Matlab Simulink. A series resonant inverter is designed which uses a pulse width modulation switching technique for controlling the inverter. A high-frequency (HF) full-bridge inverter circuit is designed and the proposed simulation diagram for the proposed system is shown in Figure 6 below as follows. In this paper, the simulation diagram contains four switches, and the switches are mainly used in the applications of producing the maximum power ratings.

In this, the MOSFET switches are taken as s1, s2, s3, and s4. On the side of the transmitter, the operation process can be divided into two cases.

Case 1: when switches 1 and 4 are switched ON that means 1 as well as it turned ON for the first half period duration and at the same time switches 2 and 3 are switched

OFF which means 0 and generate the voltage output are tends to equal to the DC voltage (Vdc) across the load.

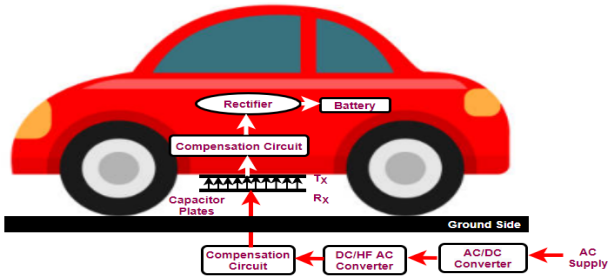

Figure 6. Proposed block diagram for the high-frequency resonant full bridge inverter

Case 2: whenever switches 2 and 3 are switched ON that means 1 and at the same time switches 1 and 4 are switched OFF. Then the voltage output tends equal to the DC voltage (Vdc). Table 1 gives a brief chart of the gating signals for the inverter output.

Table 1. Inverter output voltage gating signals

Switch 1	Switch 2	Switch 3	Switch 4	Vo(Inverter Output Voltage)
1	1	0	0	Vin
1	0	1	0	Zero
0	0	1	1	-Vin
0	1	0	1	Zero

The four MOSFETs form a full-bridge inverter configuration. Both pairs of MOSFETs S1, S2, and S3, S4 have switched alternatively with a 180-degree phase shift. For this, two pulse generators are used. Pulse generators 1, 2, and 3, 4 produce a square wave of frequency 65KHz. The duty cycle will be 50 %. During MOSFETs turn ON it acts as a switch and conducts current and transfers energy to the primary winding of the transformer. Almost all the circuits having the switching frequency are equal to the resonant frequency to get very high efficiency.

So here the switching frequency (FSW) is chosen to operate the inverter at its resonant frequency (fr) to obtain maximum efficiency. The input of the inverter is DC 12V. During the alternative conduction of one pair of MOSFETs. S1 and S2 DC passes through the primary coil of the transformer in a clockwise direction. Then the first set of MOSFETs S1 and S2 are turned OFF and the second pair of MOSFETs S3 and S4 are turned ON. Now again the DC flows through the transformer winding but in the opposite direction. Normally the switching of the MOSFETs happens only at a very high frequency. The inverter output produces the output voltage in DC of 12 V. Table 2 shows the simulation parameter specification analysis.

Table 2. Parameter specifications for the high-frequency (hf) resonant full bridge inverter

Parameter	Symbol	Value	Unit
DC input voltage	Vin	13~24	V
DC output voltage	Vo	13~24	V
Maximum input power	Pin	5.5	No
Switching frequency range	Fsw	65	kHz
Turns Ratio rating	Ntr	1:1	-
Equivalent resistive load (ERL)	RL	50 ~ 900	Ω
Duty Cycle	-	50%	-
Capacitance value	C	1Uf	F
AC input voltage	Vin	220	V

As a result of alternative switching, the varying current direction in the transformer converts the DC into AC. The AC output can be obtained from the secondary winding of the transformer. Thus, the DC input voltage of 12V is transferred into High-Frequency (HF) AC output by the half-bridge inverter. Figure 7 shows the output waveform of the gating signals.

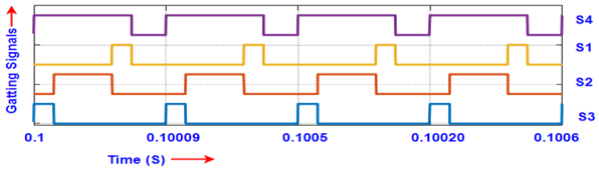

Figure 7. Proposed output gating signals

3.1 Transmitting side

The transmitter coil receives the output of the full-bridge series resonant inverter. The transmitter coil converts the HF AC voltage into an HF electromagnetic field. The field gets radiated along the vertical axis of the coil. Figure 8, 9, 10, and 11 shows the transmitted side output.

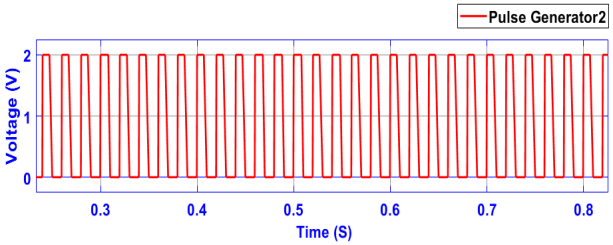

Figure 8. Pulse generator waveform on the transmitter side

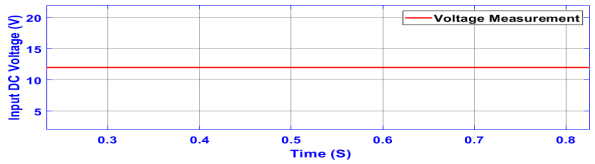

Figure 9. Input DC voltage measurement waveform in the transmitter side

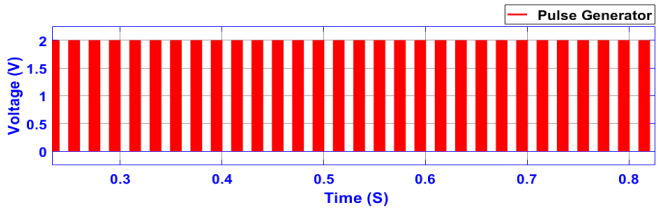

Figure 10. Transmitted pulse generator

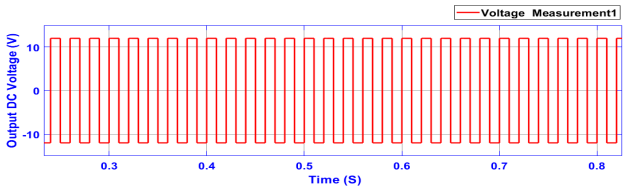

Figure 11. Voltage measurement for the input voltage of 12V

3.2 Receiver side

The receiver side has a coil that can convert the electromagnetic field back into HF AC voltage when aligned with the axis of the transmitter coil. Thus, the output of the receiving coil will be AC 12V at 65KHz. The fast-switching rectifier converts the HF AC into a DC voltage. The DC voltage is smoothened by a capacitor filter and utilized for charging and discharging the battery which is present in an electric vehicle. Figure 12,13,14 shows the output diagram for the receiver side.

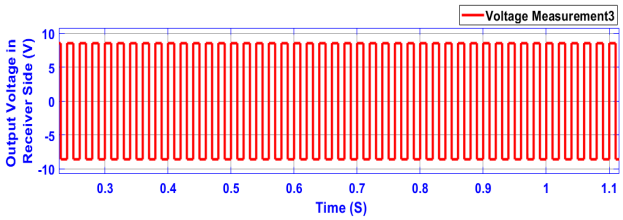

Figure 12. Voltage measurement on the receiver side

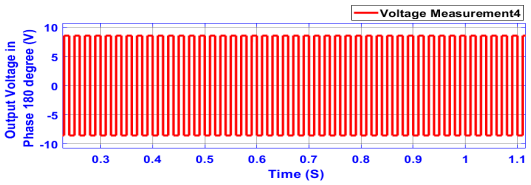

Figure 13. Output voltage measurement in phase angle 180 degrees present on the receiver side

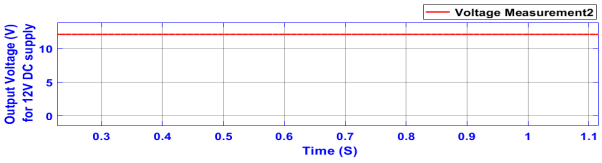

Figure 14. Output DC voltage for the input voltage of 12V on the receiver side

For finding the operation of the switching, the input DC voltage polarity and the resonance current are the most important factors to find the operation. The operation involved in the switching process is classified into four modes that depend mainly on the DC voltage polarity as well as the resonant converter current availability.

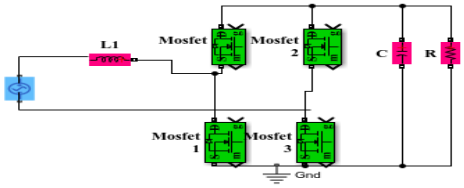

Figure 15. Proposed PWM rectifier circuit Diagram

Hence, in this operation, the given input AC electrical power must be corrected and then regulated to boost the battery voltage. When charging operation, the voltage battery needs a superficial control and operating control system due to its special characteristic while in the charging process. In this process, we have to know the appropriate secure range present in the charging state in which it is easier to charge the vehicle's battery without charging excessively or discharging [24]. Several charging techniques may be utilized to regulate, control, and alter the power that is provided to charge the battery. Thus, pulse width modulation is the most important method to generate the pulses. The main convenience of this method is to adjust, and it can be rectified without the use of any converters. The PWM can be able to process the operation with two controlled switches or with four controlled switches.

Figure 15 and 16 shows the proposed diagram using the SMPS switch. The input voltages of 12V and 24V for the high-frequency inverter are designed. The resistance load (RL) of 150 ohms is taken for the evaluated rated power of 5Kw. A capacitor filter of 100 µF is considered and modeled to obtain the controlled output voltage present across the load with a distorted output ripple of less than 2%. The output gate pulses are obtained by using the PWM technique

and by using the SMPS switch technique with their carrier frequency range of 65 kHz. When the power is flowing from the input sources to load in the circuit, the relays present namely R1 and R3 are normally turned on and the different types of duty ratios are considered.

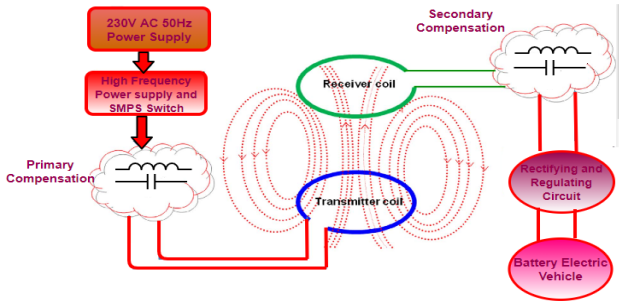

Figure 16. Proposed block diagram using SMPS switch

The duty ratios namely d1 = 20%, d2 = 49%, d3 = 20% and d4 = 80% are considered in the simulation. Then it should be evaluated in which the duty ratio d3 in mode 1 operation where the inductor is getting a charge from the source Vsc and then the charging can be continued for both sources namely (Vsc +Vs) present with the duty ratio d2 = 49% present in the mode 2 operation. Hence, in the duty ratio of d1=20% and it charges from source Vs in the mode 3 operation. In mode 4 operation, by use of the freewheeling diode, the inductor energy stored is transmitted to the load. Then the inverter produces the output voltage of 220 V across the load as depicted in the output figure. The output waveform of the simulation outcomes shows that the proposed method offers and provides power effectively from both the input sources to the load and the again load to the input source. By adjusting the value of the duty ratio, the voltage converter's output can be controlled and adjusted for the requirement of the output power of the vehicle. Figure 17 shows the waveform for voltage and current output. Figures 18 to 22 show the output waveform on the transmitter side and the receiver side.

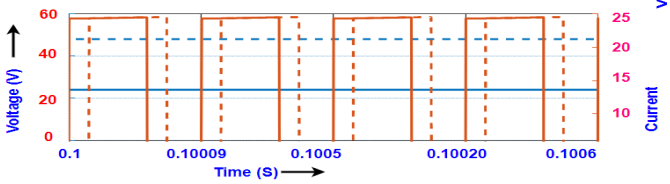

(a) Waveform for Voltage(V) and Current(A)

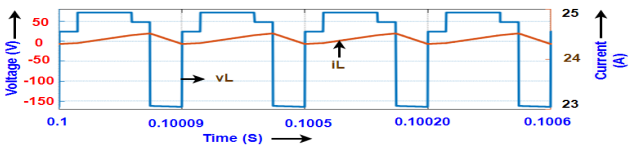

(b) Waveform for V_L and I_L

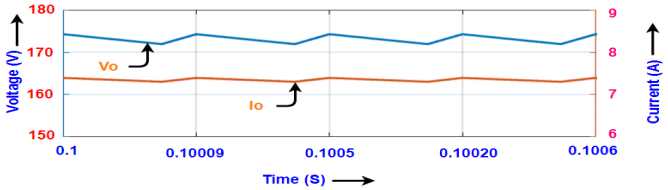

(c) Waveform for V_0 and I_0

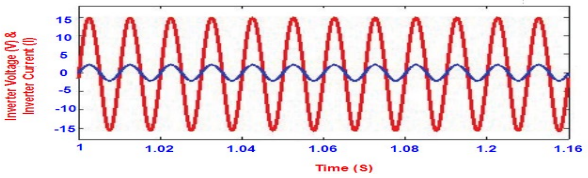

(d) Waveform for power flowing from the given input to the load

Figure 17. Simulation waveforms (a,b,c,d)

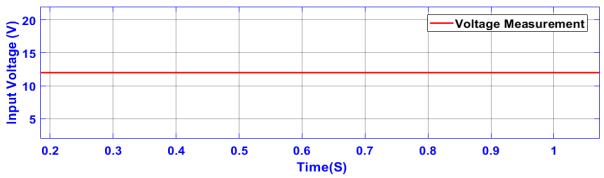

Figure 18. Voltage measurement using SMPS switch

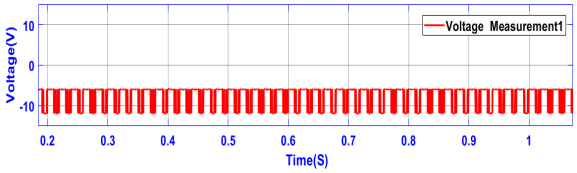

Figure 19. Pulse generator for the given input voltage

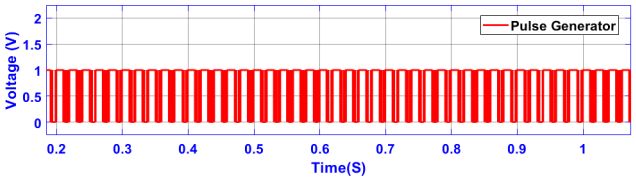

Figure 20. Pulse generator using SMPS switch

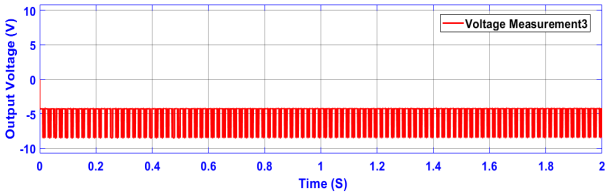

Figure 21. Output voltage waveform for the SMPS switch

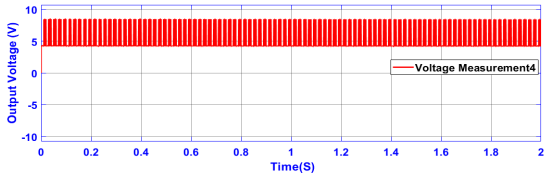

Figure 22. output voltage waveform on the receiver side

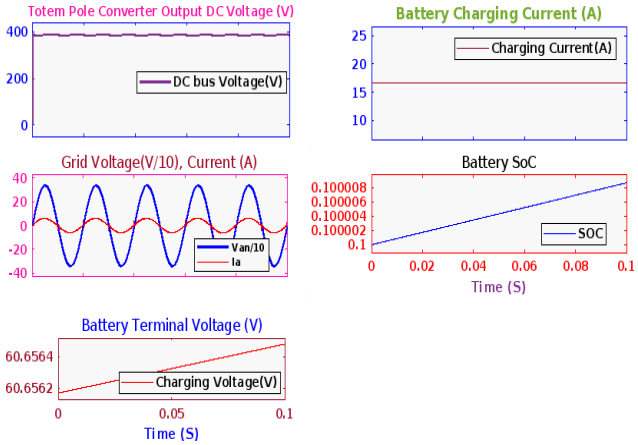

Figure 23. Converter output dc voltage, grid voltage and current, battery charging current, and terminal voltage on the receiver side

The transmission power can be evaluated based on the simulation process. Evaluated value of Pin = 182.2 W, Qin = 01, Pout = 170.7 W, Qout = 0. In this proposed system, here the reactive power obtained is 0(zero) due to the elements present in the inductance of the primary winding being appropriate another one is exactly because of this reason that the resonant circuit remains completely resistive. Figure 22,23 shows the block diagram of the battery terminal voltage, charging current, battery SoC, Grid voltage and current, efficiency, and DC power source. Table 3 depicts the comparison of the proposed and existing system as follows. Theoretically, PF and the efficiency values are evaluated as follows,

$$\eta = \frac{P_{out}}{P_{in}} = \frac{170.9}{182.9} = 95.2\% \quad (7)$$

$$DPF = \frac{P}{S} = \frac{P}{\sqrt{P^2+Q^2}} = 1 \quad (8)$$

$$PF = \frac{1}{\sqrt{1+THD^2}} . DPF = \frac{1}{\sqrt{1+0.48^2}} .1 = 0.901 \quad (9)$$

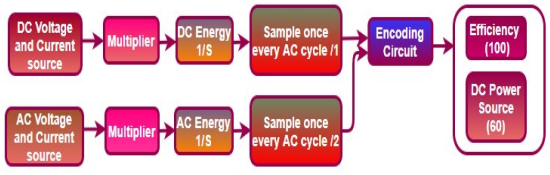

Figure 24. DC power source and efficiency block diagram

Table 3. Table of parameter comparisons between the proposed system and the existing system

Parameter Specification	Proposed system	Existing System
The voltage of the DC input	12V	24V
DC output voltage	12.12V	24.9V
Maximum input power	2287kw	1525kw
Switching frequency range	85kHz	65kHz
Turns Ratio rating	1:1:1	1:1
Equivalent resistive load (ERL)	40 ~ 800 Ω	40 ~ 800 Ω
Duty Cycle	50%	50%
Capacitance value	1.0 μf	10μf
The voltage of the AC input	230V	230V
Efficiency Range(ṅ)	96.6%	87%
Total Losses evaluated in Watts (P)	12.4w	23w

4. Conclusion

In this paper, the HF Resonant Full Bridge type Inverter for an inductive EV charging system using series resonant topology is simulated using Matlab Simulink has been proposed and developed. The proposed circuit diagram is made by using the high-frequency inverter and by using the SMPS method with an input voltage of 12V and 24V. The performance of the proposed system was verified on a 5-kW simulation type with the switching frequency at 65 kHz. This high-frequency inverter used in this proposed method has many conveniences and offers a very high-efficiency range when compared to the existing method and soft switching transition depending on the phase shift. Then the separate output waveform for the pulse generator and its analysis are evaluated. Hence, the efficiency block diagram is made for the proposed circuit diagram and attached to that to reach the maximum value of 95% for both the circuit diagram. The MOSFET full-bridge switches occupy the majority of system power loss. The VD rectifier with an output filter needs to decrease its conduction loss for further efficiency improvement at higher power. Finally, the comparison table is made for the proposed and the existing system. Then, in future work, for each coil present on the ground side, its power range rating would be improved. Additionally, a mechanical air gap would be widened between a ground-side coil buried in the ground and a vehicle-side coil through simulation and hardware implementation. Hence, to find the electric vehicle coil's distance between the transmitter and receiver, the coil's diameter and structure.

References

[1] Jan-Mou Li, Jianlin Li. Exploratory spatial distribution of dynamic wireless charging demand for EVs: Front. Energy Res.. 2019; 7(3): 126-134.

[2] Purwadi, A, Haryanto, D, Pribadi, J, Rohmatulloh, S, Hindersah, H, Haroen, Y. Modelling and Analysis of High-Frequency Inductive Power Transfer for Electric Vehicle Charging System: IEEE PELS Workshop on Emer. Tech. 2019; 61: 618-625.

[3] Al-Waeli, A, H, A, Sopian, K, Yousif, J, H, Kazem, H, A, Boland, J, Chaichan, M, T. Artificial neural network modeling and analysis of photovoltaic/thermal system based on the experimental study: Energy Convers. Manag.. 2017; 186: 368–379.

[4] Zhang, Z, Huo, H, Zhang, X. Research on three-coils magnetic coupling resonant wireless power transmission with power amplifier: IREE. 2021; 16(4): 360-367.

[5] Anyapo, C, Teerakawanich, N, Mitsantisuk, C. Development of multi-coiled dynamic wireless power transfer for electric vehicle: IREE. 2021; 17(2): 185-195.

[6] Manganiello, P, Ricco, M, Petrone, G, Monmasson, E, Spagnuolo, G. Optimization of perturbative PV MPPT methods through online system identification: IEEE Trans. Ind. Elec. 2015; 61(12): 6812-6821.

[7] Jirasuwankul, N, Klongboonjit, S, Manop, C. Effects of demand fluctuation and mitigation strategy in low voltage EV charging station by battery energy storage system: IREE. 2019; 16(5): 409-417.

[8] Yenchamchalit, K, Kongjeen, Y, Bhumkittipich, K, Stativa, A, Mithulananthan, N. Control of Low-Frequency oscillation on electrical power system under large EV-charging station installation using PSO technique for turning PSS parameters: IREE. 2020; 16(5): 401-408.

[9] Shafei, M, Salama, M, Mansour, A, Ibrahim, D. Recharging Portable devices by photovoltaic modules using inductive power transfer: IRECON. 2021; 9(5): 230-238.

[10] Carigiet, F, Knecht, R, Baumann, T, Brabec, C,J, Baumgartner, F,P. New PV system Concept: inductive power transfer for PV modules: Int. J. Euro. Photo. Sol. Ener. 2018; 172(3): 332-350.

[11] Thrimawithana, D,J, Madawala, U, K. A primary side controller for inductive power transfer systems: IEEE Int. J. Ind. Tech. 2018; 112: 661-666.

[12] Kuditi Kamalapathi, Panugothu Srinivasa Rao Nayak, Vipul Kumar Tyagi. Design and implementation of dual-source (WPT + PV) charger for EV battery charging. Energies. 2021; 31(11): 376-389.

[13] Abdelhamid, M, Singh, R, Qattawi, A, Omar, M, Haque, I. Evaluation of on-board photovoltaic modules options for electric vehicles: IEEE Journal of PV. 2020: 32(3): 334-346.

[14] Satya Prakash Oruganti, K, Aravind Vaithilingam, C, Rajendran, G, Ramasamy, A. Design and sizing of the mobile solar photovoltaic power plant to support rapid charging for electric vehicles: Energies. 2019; 12(18): 302-330.

[15] Teck Chuan Beh, Imura, T, Kato, M, Hori, Y. Basic study of improving the efficiency of wireless power transfer via magnetic resonance coupling based on impedance matching: Circuit Theory. 2016; 18: 203-215.

[16] Mirsad Hyder Shah, Nasser Hassan Abosaq. Wireless power transfer via inductive coupling: Int. J. Pow. Elec. 2020; 15(3): 2254 – 4143.

[17] Thrimawithana, D, J, Madawala, U,K. A generalized steady-state model for bidirectional IPT systems: IEEE Trans. Pow. Elec. 2016; 28(10): 4681 – 4689.

[18] Samanta, S, Rathore, A,K. Analysis and design of load-independent ZPA operation for P/S and PS/S tank networks in IPT applications: IEEE App. Elec. Phy. 2018; 14: 2470-6647.

[19] Thrimawithana, D.J, Madawala, U,K. A Generalized steady-state model for bidirectional IPT systems: IEEE Trans. Pow. Elec. 2019; 28(10): 4681-4689.